ENHANCEMENT OF THE NEAR-SIDE COMPONENT IN QUASI-ADIABATIC CALCULATIONS OF THE ^{66}Zn(d,p)^{67}Zn REACTION

E.J. Stephenson, A.D. Bacher, G.P.A. Berg, V.R. Cupps, C.C. Foster, N. Hodiwalla, P. Li, J. Lisantti, D.A. Low, D.W. Miller, C. Olmer, A.K. Opper, B.K. Park, R. Sawafta, and S.W. Wissink
Indiana University Cyclotron Facility, Bloomington, IN 47405

J.A. Tostevin, D.A. Coley, and R.C. Johnson
Department of Physics, University of Surrey, Guildford, Surrey GU2 5XH, U.K.

While mass transfer reactions are the main tool by which we study the levels of unstable nuclei, the Distorted Wave Born Approximation used to model the reaction is often inadequate to the task, compromising the value of any spectroscopic information generated. In the case of (d,p) reactions, this difficulty is often traced to the treatment of the scattering wavefunction in the deuteron entrance channel. Much of the deuteron flux goes into breakup, and coupling from the elastic channel to the breakup states is large enough to seriously modify the scattering wavefunction.

The most promising technique for treating the full complexity of the deuteron entrance channel involves coupled discretized continuum channel (CDCC) calculations,[1,2] but current calculations do not yet include an adequate treatment of the spin degrees of freedom. Thus they cannot be compared usefully with experiment. More practical calculations have been made with the adiabatic approximation,[3] which treats coupling only into relative S-wave n–p states. Comparison at intermediate energies with angular distributions of cross section, vector (A_y) and tensor (A_{yy}) analyzing power for the ^{116}Sn(d,p)^{117}Sn reaction showed, however, that adiabatic calculations are inadequate to represent the general features of the data for some cases,[3] in particular for transitions with $j = \ell - 1/2$ coupling. Further theoretical investigation of the nature of the adiabatic calculations shows that they are dominated by flux that flows around the far side of the nucleus from the detector, and that the bound neutron orbit is coplanar with the asymptotic deuteron and outgoing proton momenta.[4,5] These properties lead to angular distributions that are predicted to show little structure, and reveal simplifying relationships that should exist among several of the reaction spin observables.[4] Neither of these is experimentally observed, and the oscillation pattern in the angular distributions of the spin observables indicates interference between comparable flux travelling on both sides of the nucleus. In a detailed investigation of the nature of the missing near-side amplitude,[5] much of its strength was obtained from nearly central deuteron-nucleus collisions in which the neutron and proton separated with large relative momentum.

The adiabatic approximation assumes that the breakup states are degenerate in energy with the deuteron entrance channel, which emphasizes states with low n–p relative

momentum. This approximation was relaxed in a development by Amakawa, *et al.*, called the quasi-adiabatic approximation.[6] While the restriction to S-wave n–p states still exists, variation in the n–p center-of-mass energy is allowed. We have extended their treatment to include nucleon spin-orbit forces consistently.

In a three body model, the deuteron scattering wavefunction $\psi_{\sigma_{\rm d}}$ with spin projection $\sigma_{\rm d}$ satisfies the Schrödinger equation

$$[E - H_{\rm np} - T_R - U(r,\vec{R})]\psi_{\sigma_{\rm d}}(r,\vec{R}) = 0 \tag{1}$$

where $H_{\rm np}$ is the n–p relative Hamiltonian, T_R is the n–p center of mass kinetic energy operator, and $U(r,\vec{R})$ is the spherically-averaged sum of the neutron and proton optical potentials. Dividing the deuteron wavefunction into breakup and elastic parts yields an inhomogeneous equation for the breakup piece

$$\Big[E - H_{\rm np} - T_R - U(r,\vec{R})\Big]\psi^{bu}_{\sigma_{\rm d}}(r,\vec{R}) = \Big[U(r,\vec{R}) + (T_R - E_{cm})\Big]\psi^{el}_{\sigma_{\rm d}} \ . \tag{2}$$

CDCC calculations[2] indicate that the elastic source term in Eq. (2) is well represented by the elastic portion of a standard adiabatic model, which we extracted from the three-body adiabatic wavefunction by projecting out the deuteron bound state wavefunction $\phi^{\sigma'_{\rm d}}_{\rm d}(r)$

$$\psi^{Ad,el}_{\sigma_{\rm d}}(r,\vec{R}) = \sum_{\sigma'_{\rm d}} \phi^{\sigma'_{\rm d}}_{\rm d}(r) \int_0^\infty dr\ r^2\ \phi^{\sigma'_{\rm d}}_{\rm d}(r)\psi^{Ad}_{\sigma_{\rm d}}(r,\vec{R}) \ . \tag{3}$$

The n–p relative Hamiltonian is also replaced with an energy, which in the adiabatic approximation would have taken on the deuteron bound state energy, $-\epsilon_{\rm d}$. In the quasi-adiabatic approach, we estimate this energy from the expectation value of the Hamiltonian for the three-body adiabatic wavefunction

$$H_{\rm np}(R) \rightarrow \epsilon(R) = \frac{\langle \psi^{Ad,bu}(r,R)\phi_{\rm d}(r)|H_{\rm np}|\psi^{Ad,bu}(r,R)\phi_{\rm d}(r)\rangle}{\langle \psi^{Ad,bu}(r,R)\phi_{\rm d}|\psi^{Ad,bu}(r,R)\phi_{\rm d}(r)\rangle} \tag{4}$$

which is evaluated for each term in a partial wave expansion of the transition amplitude of the reaction. The deuteron scattering wavefunction then becomes the sum of the elastic term from the adiabatic three-body model and the breakup term from the inhomogeneous three-body equation (Eq. (2)).

Measurements[7] made previously for the ^{66}Zn(d,p)^{67}Zn ground state transition ($J^\pi = 5/2^-$) with 88.2 MeV deuterons were compared with adiabatic and quasi-adiabatic calculations. The results for the cross section and three spin observables are shown in Fig. 1. The quasi-adiabatic calculation now contains most of the oscillation pattern present in the data and absent in the adiabatic calculations. We do not expect detailed agreement since the quasi-adiabatic calculations were made in zero range, and do not include the effects of stripping from the deuteron D-state. These are a part of the adiabatic calculation, and comparing those calculations with and without the D-state contribution shows that the differences at large angle in A_y and small angle in A_{yy} originate with this change.

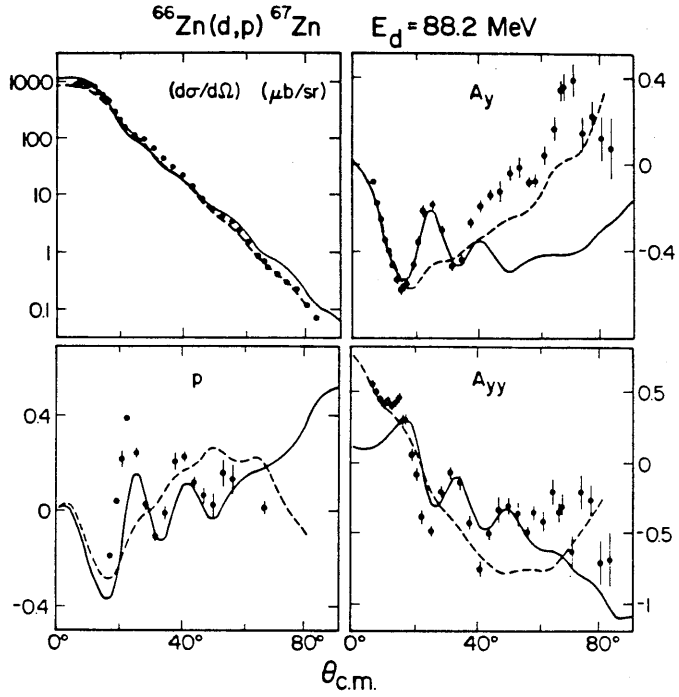

Figure 1. Angular distributions of the cross section, vector (A_y) and tensor (A_{yy}) analyzing powers, and the outgoing polarization (p) for the ^{66}Zn(d,p)^{67}Zn ground state $5/2^-$ transition. The dashed curves represent adiabatic calculations; the solid curves represent quasi-adiabatic calculations.

While the quasi-adiabatic calculation is promising as a way to understand the presence of large near-side amplitudes, the lack of detailed agreement prevents a complete evaluation of the successes of the method. Another way to examine the calculation is to divide it into near-side and far-side amplitudes, according to Eq. (2) of ref. 5. This was done for the two partial cross sections,

$$(d\sigma/d\Omega)_0 = (d\sigma/d\Omega)(1 - A_{yy})/3 \tag{5}$$

and

$$(d\sigma/d\Omega)_{-1} = (d\sigma/d\Omega)(1 - 3A_y/2 + A_{yy}/2)/3 \ , \tag{6}$$

which select out the dominant far-side amplitudes with quantum numbers $\langle m, \sigma_p | \sigma_d \rangle = \langle 5/2, 1/2|0\rangle$ and $\langle 5/2, -1/2| - 1\rangle$, respectively. Under the assumption that a single amplitude dominates each of these partial cross sections, the experimental values can be used to determine an empirical (but based on the concept of a single complex-ℓ-plane pole for each term) near-side and far-side amplitude by fitting to the form[5]

$$(d\sigma/d\Omega) = A^2\varphi^2_{\rm far} + (a^2 + \bar{a}^2)\varphi^2_{\rm near} + 2A[a\ \cos(\Lambda\theta) + \bar{a}\ \sin(\Lambda\theta)]\varphi_{\rm far}\varphi_{\rm near} \tag{6}$$

where

$$\varphi_{\rm far} = \frac{\theta^{\mu-1}}{\sqrt{\sin\theta}}\ \exp(-\Gamma\theta + \Upsilon\theta^2)$$

$$\varphi_{\rm near} = \frac{\theta^{\nu-1}}{\sqrt{\sin\theta}}\ [\exp(-\Gamma'\theta + \Upsilon'\theta^2) + R\ \exp(-\Gamma''\theta)] \ .$$

The free parameters of this empirical form (A, a, a', μ, ν, Γ, Υ, Γ', Υ', Λ, R, and Γ'') were adjusted to reproduce the experimental partial cross sections with good success, as shown in Fig. 2. In particular, the oscillation pattern that arises from near-side–far-side interference is well modelled, allowing the relative sizes of the near-side and far-side amplitudes to be estimated.

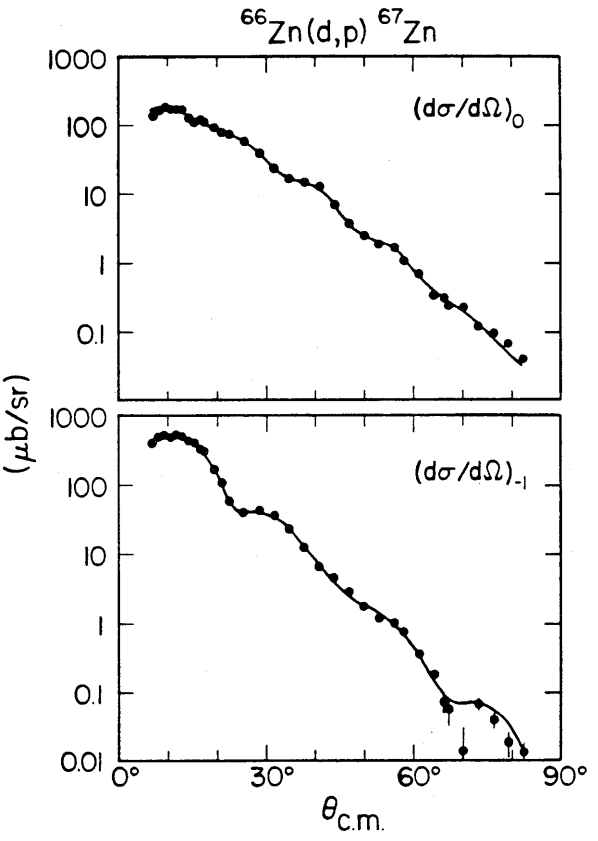

Figure 2. Angular distributions of the partial cross sections $(d\sigma/d\Omega)_0$ and $(d\sigma/d\Omega)_{-1}$ in units of μb/sr. The curves were generated using Eq. (6).

Figure 3 compares far-side and near-side amplitudes from both the adiabatic and quasi-adiabatic calculations with errors bands for the experimental amplitudes determined from the empirical fit. Good agreement is obtained for the near-side piece of $(d\sigma/d\Omega)_0$ in the middle angle regions with the quasi-adiabatic near-side amplitude. The near-side amplitude from the adiabatic calculation is too small by a factor of at least two. For $(d\sigma/d\Omega)_{-1}$ there is less difference between the adiabatic and quasi-adiabatic near-side amplitudes. Near 20°, the empirical near-side amplitude is well-determined and somewhat larger than even the quasi-adiabatic calculation.

Considerable improvement is obtained for the agreement between experiment and theory for $j = \ell - 1/2$(d,p) reactions when quasi-adiabatic deuteron scattering wavefunctions are used in the standard distorted wave theoretical model. The improvement comes about largely because of better energy sharing between the n–p relative and center-of-mass motions for the deuteron. This shift gives rise to a larger near-side amplitude, in better agreement with experiment.

1. N. Austern, Y. Iseri, M. Kamimura, M. Kawai, G. Rawitscher and M. Yahiro, Physics Reports **154**, No. 3, p. 125 (1987).
2. M. Kamimura, M. Yahiro, Y. Iseri, H. Kameyama, Y. Sakuragi and M. Kawai, Prog. Theor. Phys. Suppl. **89**, 1 (1986).
3. V.R. Cupps, J.D. Brown, C.C. Foster, W.P. Jones, D.W. Miller, H. Nann, P. Schwandt, E.J. Stephenson and J.A. Tostevin, Nucl. Phys. **A469**, 445 (1987).
4. E.J. Stephenson, R.C. Johnson, J.A. Tostevin, V.R. Cupps, J.D. Brown, C.C. Foster, J.A. Gering, W.P. Jones, D.A. Low, D.W. Miller, H. Nann, C. Olmer, P. Schwandt, J.W. Seubert and S.W. Wissink, Phys. Lett. **171B**, 358 (1986).
5. R.C. Johnson, E.J. Stephenson and J.A. Tostevin, Nucl. Phys. **A505**, 26 (1989).
6. H. Amakawa, N. Austern, and C.M. Vincent, Phys. Rev. **C29**, 699 (1984).
7. E.J. Stephenson, *et al.*, IUCF Scientific and Technical Report, May 1988 – April 1989, p. 73.

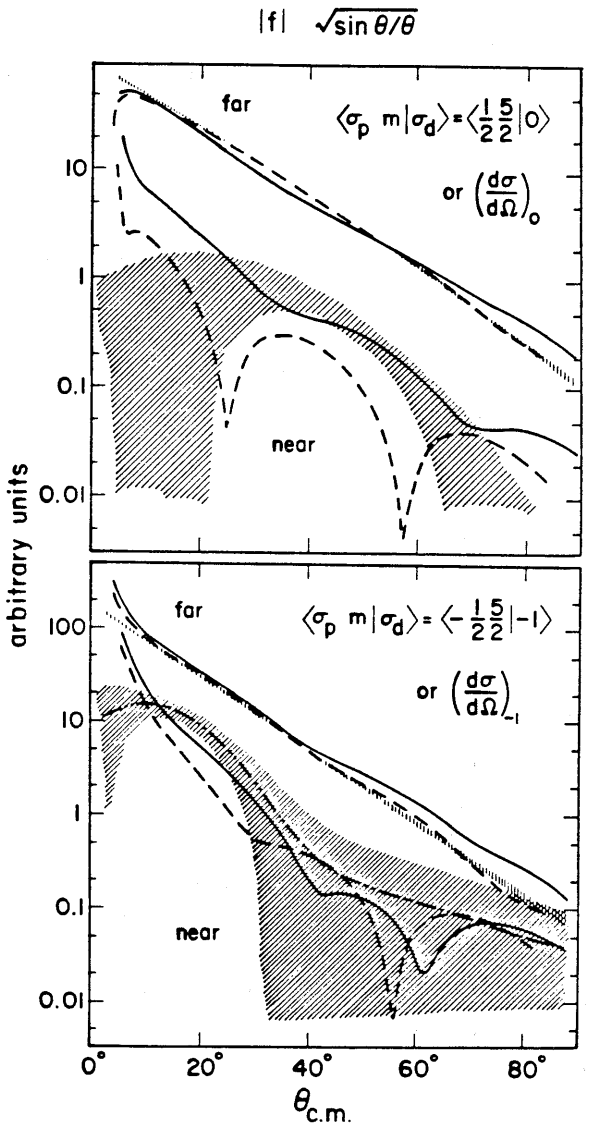

Figure 3. Angular distributions of the amplitudes $\langle m, \sigma_p|\sigma_d\rangle$ separated into far-side and near-side components. The solid (dashed) curves show this separation for the quasi-adiabatic (adiabatic) calculation. These amplitudes have been multiplied by $\sqrt{\sin\theta/\theta}$ to emphasize the linearity of the far-side component. The far-side and near-side amplitudes extracted from the partial cross section angular distributions of Fig. 2 are indicated by hashed regions that span one standard deviation above and below each amplitude. The far-side uses vertical hashing and the near-side diagonal hashing. For $(d\sigma/d\Omega)_{-1}$ a dash-double-dot line has been added for clarity to represent the experimental near-side amplitude.